COMPONENT PART NOTICE

THIS PAPER IS A COMPONENT PART OF THE FOLLOWING COMPILATION REPORT:

TITLE: Proceedings of the U.S. Army Symposium on Gun Dynamics (7th)
Held in Newport, Rhode Island on 11-13 May 1993.

TO ORDER THE COMPLETE COMPILATION REPORT, USE AD-A278 075.

THE COMPONENT PART IS PROVIDED HERE TO ALLOW USERS ACCESS TO INDIVIDUALLY AUTHORED SECTIONS OF PROCEEDING, ANNALS, SYMPOSIA, ETC. HOWEVER, THE COMPONENT SHOULD BE CONSIDERED WITHIN THE CONTEXT OF THE OVERALL COMPILATION REPORT AND NOT AS A STAND-ALONE TECHNICAL REPORT.

THE FOLLOWING COMPONENT PART NUMBERS COMPRISE THE COMPILATION REPORT:

AD#: AD-P009 060 AD#:

AD#: thru AD#:

AD#: AD-P009 091 AD#:

Accesion For	
NTIS CRA&I	☒
DTIC TAB	☐
Unannounced	☐
Justification	
By	
Distribution /	
Availability Codes	
Dist	Avail and / or Special
A-1	

DTIC FORM 463
MAR 85

OPI: DTIC-TID

SIMULATION OF TANK CANNON LAUNCH DYNAMICS

*J. Bornstein, D.S. Savick, D.H. Lyon, E.M.Schmidt
J. Kietzman & D. Deaver
U.S. Army Research Laboratory
Weapons Technology Directorate
Aberdeen Proving Ground, MD 21005-5066

ABSTRACT

Improvements have been made in a suite of computer simulations designed to model the launching of saboted, fin-stabilized projectiles from smooth bore guns. These modifications include modeling of the projectile release from the gun tube, subsequent sabot petal shape alteration because of the release of the gun tube constraints on the launch package and inclusion of more realistic initial conditions for the sabot discard model. Inclusion of these modifications has altered the resulting initial linear and angular motion of the projectile as it enters free flight from the motion reported in earlier papers. It has also modified the degree of agreement with experimental results. Additionally, mechanisms now exist within the model to provide some variability in the initial free flight projectile motion, resulting in target impact dispersions, heretofore not present in this simulation suite.

*BIOGRAPHY
PRESENT ASSIGNMENT: Aerospace Engineer, Advanced Weapons Concepts Branch, Weapons Concept Division
PAST EXPERIENCE: Aerospace Engineer, Fluid Physics Branch, BRL concerned with investigation of launch dynamics for large and medium caliber ammunition.
DEGREES HELD: PhD, Aeronautics & Astronautics, Polytechnic Institute of Brooklyn

INTRODUCTION

A principal goal of modelling the launch process for direct fire ammunition is to correctly predict the impact of rounds on target. Once this is achieved, the sensitivity of impact to variations in launch conditions can be studied for the purpose of analyzing bias and dispersion. A previous paper[1] discussed the application of a suite of computer simulations to describe the launch process for saboted 120mm tank main gun ammunition, including gun dynamics, in-bore projectile motion, and sabot discard. The primary elements of this simulation suite, also used in the current implementation, are "The Little Rascal"[2] gun and in-bore projectile Dynamics model and the AVCO sabot discard model[3] as modified by Sepri[4]. Predicted impacts for 120mm training ammunition were compared with experimental results. Discrepancies between prediction and test results were noted and suggestions for further improvements of the model, which might lead to the resolution of these disparities, were mentioned.

The current paper discusses three extensions of the earlier model. The first, developed by Kietzman[5], examines the initial stage of the sabot discard process immediately after the launch package exits the muzzle and is released from the constraint of the gun tube. At this point in the projectile trajectory, the relatively elastic sabot petals have been deformed from their initial shape through interaction with the gun tube resulting from in-bore balloting motion. Once released from the gun tube, the petals are free to return to their original, undeformed state. This latter process is referred to as sabot decompression. The resulting redistribution of energy and momentum among the individual components comprising the launch package (three or more sabot petals and the projectile) can modify both the linear and angular motion of the projectile.

In his original work, Kietzman simplified the problem by assuming that both the front and rear bore-riding surfaces are released simultaneously from the constraints of the gun tube. Given the relatively high projectile velocity at the muzzle and fairly close spacing of the two boreriding surfaces, it was presumed that the time span required for passage of the two surfaces by the muzzle would be small compared to the time required for the decompression process to finish. Subsequent computations showed that this assumption was incorrect. In the second extension, Deaver[6] modified the analysis to consider the sequential release of the front and rear bore-riding surfaces, together with the interaction between the launch package and gun tube during this transitional phase.

The final extension of the model suite is the use of a more complete set of initial conditions for the sabot discard model. In the earlier paper, it was assumed that the sabot is firmly attached to the penetrator and shares a common pitching motion during sabot discard initiation. In the current implementation, individual pitch and yaw rates are specified for each petal and a separate pitch rate is specified for the penetrator. Inclusion of projectile release from the gun, sabot decompression and more complete initial conditions for sabot discard have resulted in changes of the predicted target impact point and have modified the degree of agreement with experimental data. The sensitivity of these enhancements of the initial roll orientation of the projectile within the gun has also injected mechanisms that produce target impact dispersion.

SABOT DECOMPRESSION MODEL

During in-bore travel, projectiles are subjected to lateral loads brought about by both curvature of the bore and motion of the gun tube. At the same time, the projectile remains radially constrained, leading to elastic deformation of both the penetrator and sabot petals. The majority of this deformation normally occurs to the sabot petals. Since the forces exerted by the gun

tube upon the sabot elements are directed inward toward the centerline, the induced stress will be compressive. Once the projectile exits the muzzle, the radial constraint is removed, permitting the petals to return to their original shape and giving each sabot element a linear and angular velocity relative to the penetrator.

The model developed by Kietzman describes the situation for a projectile consisting of a rigid penetrator surrounded by three rigid sabot petals. Extension of the model for systems consisting of four or more sabot petals can, however, be easily accomplished. Following the lead of lumped parameter in-bore dynamics models, e.g., "Little Rascal", the forces resulting from interaction among the four components are modeled using six linear springs, with two springs connecting each sabot petal to the penetrator (see Figure 1). The contact points for each spring are located on the longitudinal axes of the appropriate bodies, at axial positions roughly corresponding to the locations of the front bore rider and rear obturator.

The model begins with the state of the projectile immediately before it exits the gun tube. At this stage, the sabot is represented as a solid annular body surrounding the penetrator and connected to it by the linear springs. The initial compression of each spring is determined by the location of the projectile axis with respect to the tube center. The "Little Rascal" simulation is used to provide the initial position and orientation of the projectile.

The Kietzman model assumes that the launch package is ejected from the gun tube instantaneously, i.e., the radial constraints on both bore-riding surfaces are removed simultaneously. Once this occurs, the petals are no longer connected to one another, and each petal is affected only by interaction with the penetrator. Thus, the effect of any side forces acting between sabot petals is neglected.

Another limitation of this model is the treatment of the sabot compressibility. While the overall volumes of the actual petals compress, the model assumes that all the compression effects can be described by a spring placed between a rigid body petal and a rigid body penetrator. This implies that all of the energy of sabot compression is transformed into kinetic energy of the petal and penetrator, rather than into other effects, such as deformation or vibration of the petal itself.

The mechanics of the simulation are centered about the temporal integration of equations defining Newton's second law

$$\sum F_{x_i} = m\ddot{x}_i \tag{1}$$

$$\sum F_{y_i} = m\ddot{y}_i \tag{2}$$

$$\sum F_{z_i} = m\ddot{z}_i \tag{3}$$

Euler's equations of motion ,

$$\sum M_{x_i} = I_{xx_i}\dot{\omega}_{x_i} + (I_{zz_i} - I_{yy_i})\omega_{y_i}\omega_{z_i} \tag{4}$$

$$\sum M_{y_i} = I_{yy_i}\dot{\omega}_{y_i} + (I_{xx_i} - I_{zz_i})\omega_{z_i}\omega_{x_i} \tag{5}$$

$$\sum M_{z_i} = I_{zz_i}\dot{\omega}_{z_i} + (I_{yy_i} - I_{xx_i})\omega_{x_i}\omega_{y_i} \tag{6}$$

and the orientation of each body in space

$$\dot{\psi}_i = (\omega_{y_i} \sin\phi_i + \omega_{z_i} \cos\phi_i) \sec\theta_i \tag{7}$$

$$\dot{\theta}_i = \omega_{y_i} \cos\phi_i - \omega_{z_i} \sin\phi_i \tag{8}$$

$$\dot{\phi}_i = \omega_{x_i} + (\omega_{y_i} \sin\phi_i + \omega_{z_i} \cos\phi_i) \tan\theta_i \tag{9}$$

for each of the four bodies considered in the simulation. The parameters ψ, θ, and ϕ represent Euler angles describing the rotation of a point from the inertial coordinate system into the non-inertial body fixed systems employed within the simulation and are chosen as a "3-2-1" system.

To simplify the integration process, multiple coordinate systems are used. The majority of the computations and the reporting of results is done in an inertial system. For convenience, the current version of the model employs the same coordinate system as the Little Rascal model. Four separate body-fixed coordinate systems have also been defined to simplify the computation of angular velocities. Each of these coordinate systems is centered at the body center of gravity (c.g.).

For the integration process, the system of equations is reformulated into a system of 48 first order differential equations, 12 equations describing the motion of each of the 4 bodies. The model uses the IMSL subroutine DIVPRK[7], which employs fifth and sixth order Runge-Kutta-Verner methods to solve the initial value problem. In its current configuration, a complete run for the model requires a few minutes time on a VAX8600 operating in a multi-user environment. Since there are no external forces acting upon the system, checks for the conservation of linear momentum, angular momentum, and total energy are performed at each time step to ensure the correctness of the integration process.

APPLICATION OF THE SABOT DECOMPRESSION MODEL

A series of computations was performed for an XM866 fin stabilized, discarding sabot training practice (TPFSDS-T) round fired from the 120mm M256 main gun of an M1A1 tank. Three cases were examined, each representing one of the three gun tubes discussed in the original paper by Lyon et al. Results from the "Little Rascal" in-bore projectile dynamics model were used to provide initial conditions. For the simulation, the flight body mass was 2.73 kg, the total launch package mass was 5.43 kg and the c.g. was 0.216 meter from the projectile base. These values differ somewhat with those used in the earlier paper but more closely represent measured values.

In both the in-bore dynamics and sabot decompression models, the interaction between each sabot and the penetrator is assumed to take place at a single contact point rather than spread over a circular arc. Thus, the compression of the individual springs will vary as the initial roll angle is modified, changing the magnitude and direction of the net forces initially acting upon the penetrator and affecting projectile trajectories once the sabots are decompressed. This apparently artificial variation of force is, to some degree, mirrored in reality. Lyon[8] has shown that the force-displacement relationship at the forward and rear bore riders of real sabots depends on the roll orientation of the sabot, i.e., location of the interfaces between petals.

Based upon the simulation results, the complete decompression process, from the point that the front bore rider exits the gun until the sabot attains its initial undeformed state, requires approximately 0.5 ms for a 120mm saboted training round. Some variation in this figure does

occur because of differing initial sabot deformation brought about by differing in-bore trajectories, gun-tube bore straightness profiles and initial roll orientation, does occur. The sabots should be fully decompressed when the projectile is approximately 0.8 meter downrange.

Sabot decompression has a negligible effect upon the axial penetrator velocity component (u). It does, however, have a measurable impact upon both transverse components. For example, the vertical velocity component for an XM866 round launched from gun #104 varies between 0.71 m/s and 0.95 m/s. This differs substantially from the initial muzzle value of 0.58 m/s, that was used in earlier simulations. In the horizontal direction, the velocity varies between -0.65 m/s and -1.0 m/s compared with a value of -0.76 m/s at the muzzle.

Figure 2 displays the trajectories of rounds launched from the three gun tubes used in the earlier paper of Lyon et al. For purposes of comparison, the experimentally measured values at a point 1.8 meters downrange have also been included. It should be noted, however, that at the 1.8 meter downrange position, sabot discard disturbances may already be having some effect upon projectile motion. Also, in the experimental measurements, a muzzle bore telescope was used to orient the gun in the range coordinate system. The telescope has mounting feet approximately 70 mm and 301 mm uprange from the muzzle when the unit is fully seated in the gun tube. The local slope of each gun tube at those points was used to rotate the simulation results into a coordinate system consistent with the measurements. This convention will be used in the further comparisons of simulation and experimental results.

From the figure, it is apparent that the decompression process adds not only a bias but also a variability to the projectile trajectory. The introduction of a large variability is especially true in the cases of guns 84 and 85 which, as noted by Lyon et al., contain significant bore curvatures. The large curvature results in major in-bore accelerations of the launch package, with subsequent deformation of the sabot petals. By lumping all the compressibilty of each sabot petal along a single axis (represented by the spring), there is a tendency for the simulation to enhance the influence of initial roll orientation. Although differences exist between trajectories determined by simulation and those reported from experiments, the simulations do tend to follow the trends seen in the test results, suggesting that it captures many of the essential elements of the actual physical processes.

Projectile angular rates are also affected by the decompression process. Figure 3 depicts the rates predicted by the simulation, together with the rates determined from measurement. Here, the agreement between simulation and reality is far less encouraging, suggesting that a more detailed model is required.

PROJECTILE RELEASE MODELING

One of the principal assumptions in the original sabot decompression model was that one could allow both the front and rear bore-riding surfaces of the launch package to be simultaneously released from the constraints of the gun tube. This was based upon the presumption that the decompression process would be relatively long compared with the elapsed time between passage of the two bore-riding surfaces by the muzzle. Unfortunately, this is not truely the case. For the cases currently being examined, decompression requires approximately 500 microseconds while the rear bore rider passes the muzzle roughly 90 microseconds after the front bore rider. Thus for a appreciable portion of the decompression process, the front of each sabot petal is free to move in space, while the rear portion is still constrained and driven by the motion of the gun.

Deaver modified the original model by dividing the sabot decompression into a two-stage process. The initial phase begins as the front bore-riding surface reaches the muzzle and lasts until the rear obturator reaches the muzzle. During this stage, the front spring between each sabot element and the penetrator is permitted to decompress and the front portion of each sabot is permitted to interact only with the penetrator. At the same time the rear portion of the launch package is treated as a single solid body, constrained to follow the motion of the gun tube. Given the relative masses of gun tube and launch package, it is assumed that the gun motion will be determined primarily by its vibrational characteristics and that the solutions obtained by the lumped parameter gun dynamics models, which do not treat the release process, remain valid. During the second phase of the model, both front and rear bore-riding surfaces are free of the gun, and the model proceeds according to the original formulation of Kietzman.

Figures 4 and 5 depict the projectile trajectory and angular motion after sabot decompression, as obtained using the modified version of the model. Comparison with Figures 2 and 3 indicates that while introduction of sequential release of the front and rear bore-riding surfaces has increased the variability of linear and angular motion with roll orientation, it has not drastically altered projectile behavior. Thus, some other aspect of the model must be responsible for its inability to reproduce the angular rate of the projectile.

SABOT DISCARD MODEL

The AVCO sabot discard code describes the flight dynamics of the sabots and projectile and calculates the forces and moments acting on the projectile. The flight dynamics are affected by sabot interactions with the projectile. If the forces and moments are distributed asymmetrically around the projectile, the penetrator flight path will be disturbed. Three types of interactions are considered in the code. First is the contact or mechanical interaction that occurs as the sabot pivots off the projectile. Second is the aerodynamic interaction caused by pressure variations because of the sabot shock waves impinging on the projectile. Third is aerodynamic interaction caused by the sabots as they lift off and temporarily shield the fins from the oncoming flow causing an uneven pressure distribution across the control surfaces.

The code requires a number of parameters to make the necessary calculations. These include the geometry of the sabot, the initial position of the sabot segments with respect to the penetrator, the aerodynamic coefficients for the bodies and their inertial properties.

The version of the code used in the earlier paper by Lyon et al assumed that penetrator and sabot initially behaved as a single rigid body which could possess only a pitching motion. This should approximate the expected behavior of an inelastic, saboted round, subject to in-bore balloting motion, as it exits the muzzle. For those simulations, the projectile pitch rate was provided by the gun dynamics codes Rascal and SHOGUN[9].

The current version of the discard model permits each of the individual sabot petals to have both a linear and angular velocity with respect to the penetrator. Thus, the sabot and penetrator can act as elastic bodies within the gun, storing energy through compression of the sabot petals and ultimately causing motion of the petals with respect to the penetrator as the energy is released when the round leaves the tube.

While the sabot petals can have independent linear velocities and rates at the outset of the integration process, it is assumed that the position and orientation of each petal with respect to the

penetrator are identical to those found before the round was launched. Strictly speaking, there is an improper matching of conditions between the sabot decompression code and the discard model. However, given the small magnitudes of the angles and offsets between the penetrator and sabot elements given by the decompression code, the error introduced was presumed to be small.

Both versions of the program yield two output parameters that are used to compute the total projectile jump: $\dot{\alpha}$, the angular rate of the projectile, and α, the c.g. trajectory of the projectile. The parameters are computed by integrating the forces and moments applied to the projectile. Results obtained through the application of the code are discussed in the following section.

COMPARISON WITH EXPERIMENTAL RESULTS

To evaluate the ability of the model to accurately predict target impact and the magnitude of the intermediate disturbances acting upon the projectile, comparisons were made with earlier experimental data for XM866 projectiles fired from an M1A1 tank. In its current configuration, the sabot discard code is limited to the treatment of cases for which the initial angular motion of the penetrator is a pure pitching motion. Thus, only two computations were performed for each of the three gun tubes considered in the investigation: one case in which the projectile was pitching up and another in which it was pitching down. For each gun tube these two situations occur for roll orientations that are approximately, though not exactly, 180° apart.

Figure 6 presents a comparison of the target impacts predicted by the current version of the simulation suite with the results of the earlier paper and the centers of impacts obtained from test firings XM866 projectiles from those gun tubes[1]. Two features become immediately apparent. First is an increased spacing between impact locations as a function of gun tube. For example, the impacts for rounds launched from gun #85 have moved over 0.5 mil toward the left, somewhat closer to the center of impacts from firing exercises. Second is the large variation of impact point for projectiles launched from the same gun tube but with differing initial roll orientation. This is particularly noticeable for the projectiles fired from gun tube #84.

To determine which of the simulation program modifications has provided the more significant contribution to the observed change in projectile impact location, the simulation was run with the sabot decompression program (simultaneous release), but with the older version of the sabot discard code, which only permits a uniform initial pitching motion for both the penetrator and sabot petals. The results of this computation for projectiles fired from gun #84 is shown in Figure 7. At least for this case, it can be clearly seen that the addition of the sabot decompression code minimally altered the trajectory of the projectile. This suggests that the introduction of asymmetrical initial conditions for the discard code had the greatest impact. The initial conditions are, however, the result of the decompression code, albeit indirectly. Additionally, the sabot decompression process contributes substantially to the angular projectile motion (though discrepancies between computed and measured values exist). Thus, it is difficult to say which model extension has made the greater contribution to the changes in the predicted impact location.

Finally, while the impact locations predicted by the simulation have moved toward the impacts measured during test firings, significant differences between the two values still exist, implying that the current model still does not fully capture the physics of the launch process.

CONCLUDING REMARKS

This paper has discussed an extension of the suite of models being used at the U.S. Army Research Laboratory to quantitatively describe the launch dynamics of large caliber ammunition for direct fire weapons. The extension has considered the process by which sabot petals, deformed by in-bore balloting motion, decompress once the constraints of the gun tube are released, causing the relative motion between each of the petals and the flight body. It has also used an improved version of the AVCO sabot discard code which permits the initial state of the projectile to include the relative motion of the penetrator and sabot petals. While the results obtained by using this improved version of the model show somewhat better agreement with experiment than the previously reported model, room for further improvement exists.

REFERENCES

[1] Schmidt, E.M., Savick, D.S., Lyon, D.H. & Plostins, P., 1990, "Comparison of Computed and Measured Jump of 120mm Cannon," Sixth U.S. Army Gun Dynamics Symposium.

[2] Erline, T.F.,Kregel, M & Pantano, M., 1990, "Gun and Projectile Flexural Dynamics Modeled by 'The Little Rascal' - A User's Manual," Technical Report 3122, U.S. Army Ballistic Research Laboratory, Aberdeen Proving Ground, MD (July).

[3] Siegelman & Crimi, P.,1979, "Projectile/Sabot Discard Aerodynamics," 1979, Contractor Report CR-00410, U.S. Army Ballistic Research Lab, Aberdeen Proving Ground, MD (Dec).

[4] Sepri, P., 1986, "Aerodynamic Interaction Between Projectile Fins and Sabot Petals," U.S. Army Ballistic Research Lab, Aberdeen Proving Ground, MD 21005 (Sept).

[5] Kietzman, J.W., "Sabot Decompression and its Effect upon the Angular Rates of APFSDS Sabots and Penetrators," U.S. Army Research Laboratory, Technical Report in preparation

[6] Deaver, D., "Private Communication"

[7] IMSL, Inc, 1987, Math/Library User's Manual, pp. 633-639.

[8] Lyon, D.H. "Radial Stiffness of Several 120mm Projectiles," Technical Report to be published, U.S. Army Ballistic Research Laboratory, Aberdeen Proving Ground, MD.

[9] Hopkins, D.A., "Modeling Gun dynamics with Three- Dimensional Beam Elements," Sixth U.S. Army Symposium on Gun Dynamics, 1990

LIST OF SYMBOLS

F	force
M	moment
m	mass
u,v,w	x,y & z velocity components
X,Y,Z	coordinates in the inertial coordinate system
x,y,z	coordinates in the body-fixed coordinate system
α	projectile pitch angle
ψ, θ, ϕ	Euler angles
ω	angular velocity

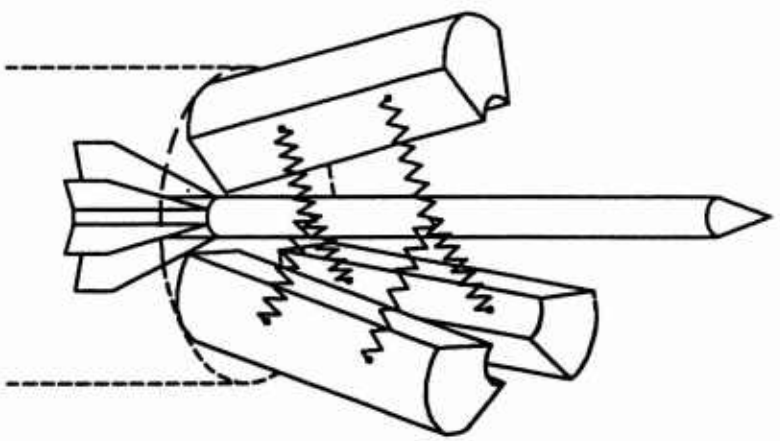

Figure 1. Geometry of projectile used for sabot decompression model

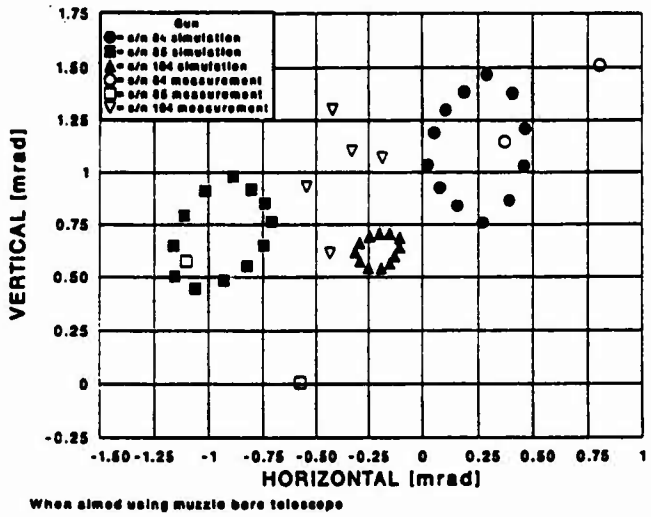

Figure 2. Projectile trajectories after sabot decompression – Kietzman model.

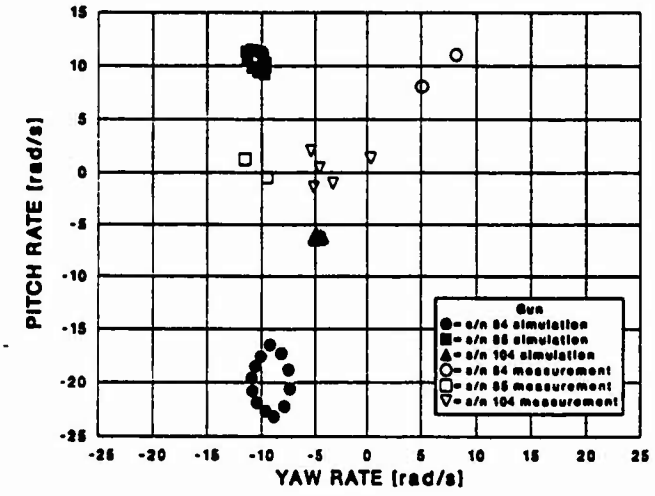

Figure 3. Projectile angular velocity after sabot decompression – Kietzman model

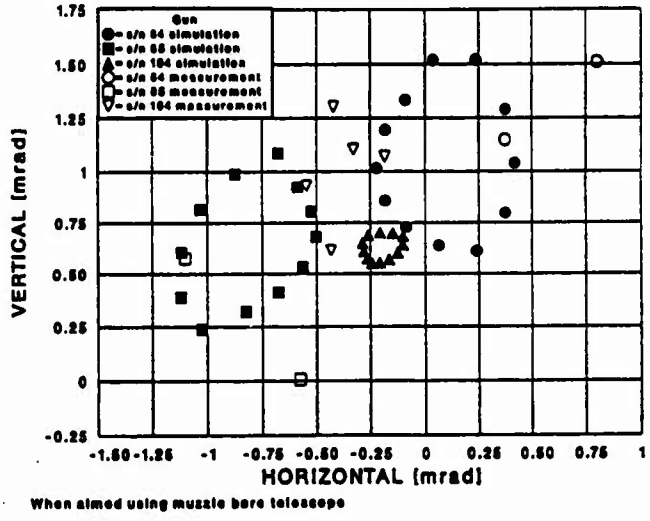

Figure 4. Projectile trajectories after sabot decompression – with sequential release of front and rear bore-riding surfaces.

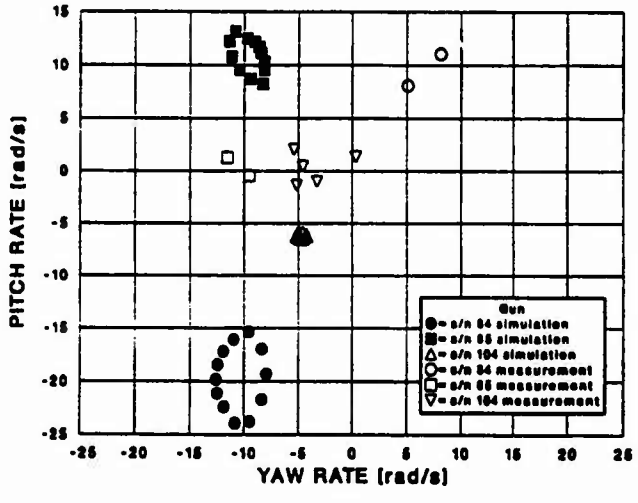

Figure 5. Projectile angular velocity after sabot decompression – with sequential release of front and rear bore-riding surfaces.

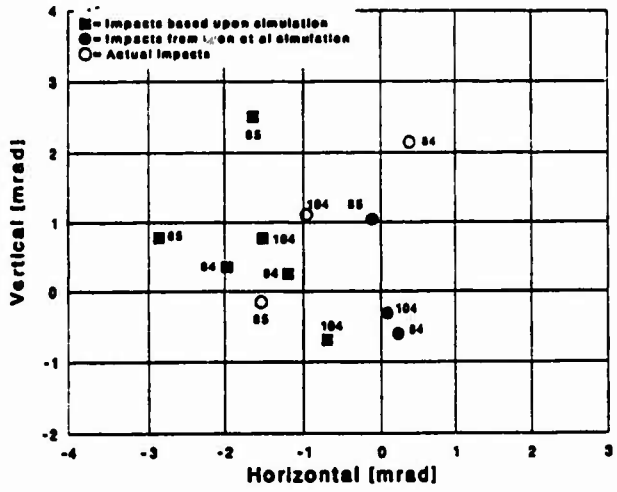

Figure 6. Comparison of impacts obtained from simulation and test firings.

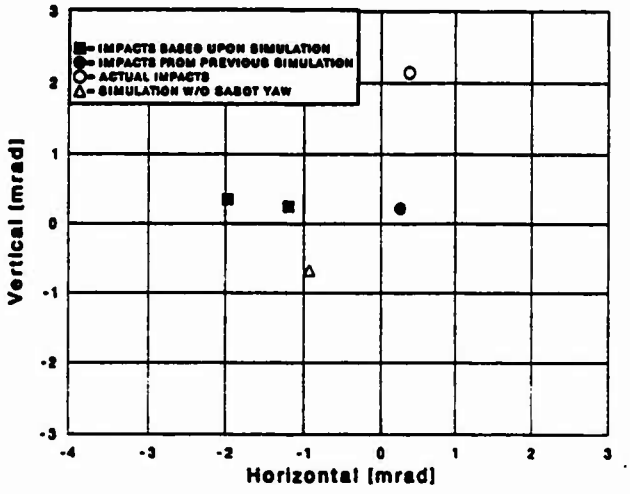

Figure 7. Comparison of impacts obtained for rounds launched from gun #84, using different simulation suites.